

Combining inherent knowledge of vision-language models with unsupervised domain adaptation through self-knowledge distillation

Thomas Westfechtel¹, Dexuan Zhang¹, Tatsuya Harada^{1,2}

¹The University of Tokyo ²RIKEN
Tokyo, Japan

{thomas, dexuan.zhang, harada}@mi.t.u-tokyo.ac.jp

Abstract

Unsupervised domain adaptation (UDA) tries to overcome the tedious work of labeling data by leveraging a labeled source dataset and transferring its knowledge to a similar but different target dataset. On the other hand, current vision-language models exhibit astonishing zero-shot prediction capabilities. In this work, we combine knowledge gained through UDA with the inherent knowledge of vision-language models. In a first step, we generate the zero-shot predictions of the source and target dataset using the vision-language model. Since zero-shot predictions usually exhibit a large entropy, meaning that the class probabilities are rather evenly distributed, we first adjust the distribution to accentuate the winning probabilities. This is done using both source and target data to keep the relative confidence between source and target data. We then employ a conventional DA method, to gain the knowledge from the source dataset, in combination with self-knowledge distillation, to maintain the inherent knowledge of the vision-language model. We further combine our method with a gradual source domain expansion strategy (GSDE) and show that this strategy can also benefit by including zero-shot predictions. We conduct experiments and ablation studies on three benchmarks (OfficeHome, VisDA, and DomainNet) and outperform state-of-the-art methods. We further show in ablation studies the contributions of different parts of our algorithm.

1. Introduction

Deep neural networks have advanced the field of computer vision largely. However large amount of labeled data is required to train these networks. One method to overcome the need for tedious labeling is unsupervised domain adaptation, where knowledge from a similar but distinct labeled source dataset is transferred to an unlabeled target dataset.

On the other hand, vision-language models exhibit re-

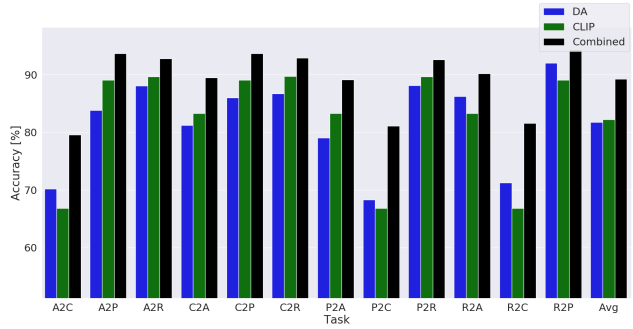


Figure 1. Accuracy on the OfficeHome dataset for unsupervised domain adaptation (blue), CLIP zero-shot predictions (green), and our combined version (black) integrating zero-shot predictions into UDA. In this work, we present a way to combine the knowledge from vision-language models with knowledge transferred via UDA from a source domain. It can be seen that the performance significantly improves.

markable zero-shot prediction accuracy, even without any task-specific training data. It may even seem that through generating larger foundation models the need for domain adaptation fades. For example, on the DomainNet dataset, current vision-language models outperform state-of-the-art domain adaptation methods while only using zero-shot predictions.

In this work, we argue that rather than seeing these two methods as competing, combining the strengths of both of them achieves even better results. We combine the inherent knowledge of the vision-language models with the knowledge transferred from a source dataset through domain adaptation.

To maintain the inherent knowledge of the vision-language model we employ a knowledge distillation loss using the zero-shot predictions. However, since the zero-shot predictions usually exhibit a large entropy, meaning that the class probabilities are rather evenly distributed, we first adjust the distribution to accentuate the winning prob-

ability. To keep the relative confidence of the zero-shot prediction between source and target data we do this step for source and target data in a combined way. We use the knowledge distillation loss, to maintain the inherent knowledge, in combination with a conventional unsupervised domain adaptation method to benefit from the knowledge of the source dataset. As can be seen in Fig. 1 combining the two knowledge sources significantly increases the performance. We further combine our method with a gradual source domain expansion strategy (GSDE) [30] and show that this strategy can also benefit by including zero-shot predictions.

Our main contributions are:

- We introduce self-knowledge distillation to maintain inherent knowledge of vision-language models using recalibrated zero-shot predictions and combine them with a conventional UDA method.
- We further employ a gradual source domain expansion (GSDE) and enhance the strategy by introducing zero-shot predictions into it.
- We show the effectiveness of our algorithm on three datasets (Office-Home, VisDA, and DomainNet) and further evaluate the method in various ablation studies.
- We show that the method is applicable for both CNN-based and transformer-based backbones.

2. Related works

2.1. Unsupervised domain adaptation

The goal of unsupervised domain adaptation is to overcome the domain shift between the source and the target dataset. Surveys for this task can be found in [41], [38]. One approach is to align the feature space distributions between the two datasets. Domain-adversarial neural network (DANN) [5] introduces an adversarial approach to achieve this. A domain classifier is trained to distinguish the feature space of source and target samples. The work introduced a gradient reversal layer. This layer inverts the gradients and thereby inverts the training objective, meaning that the backbone is trained to generate features that are indistinguishable for the domain classifier, generating so-called domain invariant features. BIWAA introduces a feature re-weighting approach based on their contribution to the classifier. CDAN [15] extended DANN by multilinear conditioning the domain classifier with the classifier predictions. Moving semantic transfer network [32] introduced a moving semantic loss.

Another approach employs information maximization or entropy minimization to generate more accurate target predictions. SHOT [14] exploits both information maximization and self-supervised pseudo-labeling to increase the performance of the target domain. SENTRY [21] uses prediction consistency among different augmentations of an im-

age to either minimize its entropy or maximize it in case of inconsistent predictions.

Following the rise of vision transformers, approaches specially tailored for these backbones have gained popularity. TVT [34] introduced a Transferability Adaption Module that employs a patch-level domain discriminator to measure the transferability of patch tokens, and injects learned transferability into the multi-head self-attention block of a transformer. CDTrans [33] introduced a triple-branch transformer framework with cross-attention between source and target domains. PMTrans [40] introduced PatchMix which builds an intermediate domain by mixing patches of source and target images. The mixing process uses a learnable Beta distribution and attention-based scoring function to assign label weights to each patch.

In our work, we employ CDAN [15] as our domain adaptation loss. While the performance is neither state-of-the-art for CNN-based nor transformer-based networks, it achieves reasonable performance for both architectures. [11] has shown that many algorithms developed for CNN backbones underperform for transformer-based backbones. On the other hand, most transformer-based algorithms explicitly make use of the network structure and cannot be employed for CNN-backbones.

2.2. Vision-language models

CLIP [22] introduced a contrastive learning strategy between text and image pairs. It employs a text encoder and a visual encoder. Feature representations of positive pairs are pushed together, while unrelated or negative pairs are pushed apart. The usage of visual and language encoders enables zero-shot prediction. The class labels are encoded via the language encoder and serve as classifier. Usually, the class labels are combined with a pretext or ensemble of pretexts such as 'A photo of a {object}.' to enhance the performance, where {object} is replaced with the respective classes. While CLIP collected the training dataset by constructing an allowlist of high-frequency visual concepts from Wikipedia, ALIGN [9] does not employ this step, but makes up for it by using a much larger, though noisier, dataset. BASIC [20] further increased the zero-shot prediction capabilities by further increasing data size, model size, and batch size. LiT [36] employs a pre-trained image encoder as visual backbone and aligns a text encoder to it. The vision encoder is frozen during the alignment. DFN [4] investigates data filtering networks to pool high-quality data from noisy curated web data.

In our work, we employ the CLIP pre-trained models due to their popularity. We employ the seven ImageNet templates subset published on the CLIP Git Hub.

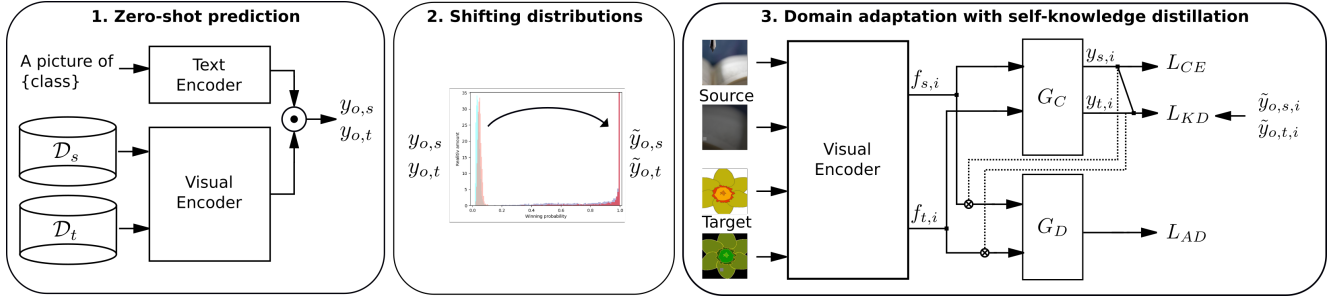


Figure 2. Process flow of our algorithm. In a first step, the zero-shot predictions of source \mathcal{D}_s and target \mathcal{D}_t dataset are estimated. The zero-shot distributions are calibrated jointly to accentuate the winning probability. The network is trained using a classification loss L_{CE} for the source data, a knowledge distillation loss employing the shifted zero-shot predictions \tilde{y}_o , and an adversarial adaptation loss L_{AD} . We further employ strongly augmented versions of source and target data as input. Since we do not differentiate between weakly and strongly augmented versions for the losses, their paths are combined after the visual encoder.

2.3. Domain adaptation for vision-language models

Surprisingly there has not been much research on combining domain adaptation to vision-language models.

Few approaches make use of prompt learning [39]. This approach trains the prompt’s context words for the text encoder with learnable vectors while the encoder weights are frozen. DAPL [7] employs a prompt learning approach to learn domain-agnostic context variables and domain-specific context variables for unsupervised domain adaptation. This approach freezes the text and vision encoder during training. AD-CLIP [25] introduces a prompt learning scheme that entirely leverages the visual encoder of CLIP and introduces a small set of learnable projector networks. MPA [2] takes a similar approach of prompt learning for multi-source unsupervised domain adaptation. In a first step, individual prompts are learned to minimize the domain gap through a contrastive loss. Then, MPA employs an auto-encoding process and aligns the learned prompts by maximizing the agreement of all the reconstructed prompts. DALL-V [35] employs large language-vision models for the task of source-free video domain adaptation. They distill the world prior and complementary source model information into a student network tailored for the target. This approach also freezes the vision encoder and only learns an adapter on top of the vision encoder.

Unlike all of the above methods, we do not freeze the vision encoder during the training. Particularly, we employ the zero-shot predictions and use them in a knowledge distillation step to retain the knowledge of the language-vision model. Furthermore, we combine our method with a conventional UDA approach.

3. Methodology

In unsupervised domain adaptation, the goal is to transfer knowledge from a source dataset \mathcal{D}_s consisting of n_s labeled images $\mathcal{D}_s = (x_{i,s}, y_{i,s})_{i=1}^{n_s}$ to an unlabeled target

dataset \mathcal{D}_t containing n_t unlabeled data $\mathcal{D}_t = (x_{i,t})_{i=1}^{n_t}$. In this work we focus on combining the inherent knowledge of vision-language models with the knowledge gained from the knowledge transfer of the source domain, meaning we further have access to the zero-shot predictions y_o for each sample.

For the knowledge transfer from the source to the target domain, we employ the widely established adversarial domain adaptation method CDAN as it was shown to be effective for both convolutional- and transformer-based network architectures [11].

To preserve the inherent knowledge of the vision-language model we employ a knowledge distillation loss [8] using the zero-shot predictions. However, since the zero-shot predictions exhibit a relatively wide spread of probabilities among the classes (see Fig. 3), we first adjust the distribution to accentuate the winning probabilities, so that they are more informative for the knowledge distillation loss. The process flow of our algorithm can be seen in Fig. 2

We further employ data augmentation and a gradual source domain expansion strategy to further boost the performance.

For a single run, we use the three losses:

$$L = L_{CE} + L_{KD} + L_{AD} \quad (1)$$

where L_{CE} is the classification loss for the source data, L_{KD} is the knowledge distillation loss, and L_{AD} is the adversarial adaptation loss. L_{KD} and L_{AD} are calculated for both source and target data. We further employ a strongly augmented version of source and target data, which are handled in the same way as the weakly augmented versions.

3.1. Knowledge distillation loss

Vision-language models already achieve an incredible zero-shot accuracy for unseen data. To preserve this knowledge we employ a knowledge distillation loss. However, since

Table 1. Accuracy results on Office-Home dataset. The best results are displayed in bold and the runner-up results are underlined. Methods using a ResNet-50 backbone are on top, and methods using a transformer-based backbone are on the bottom. ZS indicates zero-shot results of CLIP.

Method	A→C	A→P	A→R	C→A	C→P	C→R	P→A	P→C	P→R	R→A	R→C	R→P	Avg
CDAN [15]	50.7	70.6	76.0	57.6	70.0	70.0	57.4	50.9	77.3	70.9	56.7	81.6	65.8
SRDC [27]	52.3	76.3	81.0	69.5	76.2	78.0	68.7	53.8	81.7	76.3	57.1	85.0	71.3
BIWAA-I [29]	56.3	78.4	81.2	68.0	74.5	75.7	<u>67.9</u>	56.1	81.2	75.2	60.1	83.8	71.5
Sentry [21]	61.8	77.4	80.1	66.3	71.6	74.7	66.8	63.0	80.9	74.0	66.3	84.1	72.2
GSDE [30]	57.8	80.2	81.9	71.3	78.9	80.5	67.4	57.2	<u>84.0</u>	76.1	62.5	85.7	73.6
PCL [12]	60.8	79.8	81.6	70.1	78.9	78.9	69.9	60.7	83.3	<u>77.1</u>	66.4	<u>85.9</u>	74.5
ZS [22]	48.5	<u>81.2</u>	<u>83.5</u>	<u>72.6</u>	<u>81.2</u>	<u>83.5</u>	<u>72.6</u>	48.5	83.5	72.6	48.5	81.2	71.5
SKD (Ours)	<u>61.6</u>	86.8	86.7	78.0	87.4	86.8	77.3	<u>61.0</u>	87.1	79.6	<u>64.1</u>	88.9	78.8
CDAN [15]	62.6	82.9	87.2	79.2	84.9	87.1	77.9	63.3	88.7	83.1	63.5	90.8	79.3
TVT [34]	74.9	86.8	89.5	82.8	88.0	88.3	79.8	71.9	90.1	85.5	74.6	90.6	83.6
CDTrans [33]	68.8	85.0	86.9	81.5	87.1	87.3	79.6	63.3	88.2	82.0	66.0	90.6	80.5
SDAT [23]	70.8	87.0	90.5	85.2	87.3	89.7	84.1	70.7	90.6	88.3	75.5	92.1	84.3
SSRT [26]	75.2	89.0	91.1	85.1	88.3	89.9	85.0	74.2	91.2	85.7	78.6	91.8	85.4
PMTTrans [40]	81.3	<u>92.9</u>	92.8	<u>88.4</u>	<u>93.4</u>	93.2	<u>87.9</u>	<u>80.4</u>	93.0	<u>89.0</u>	<u>80.9</u>	94.8	<u>89.0</u>
ZS [22]	66.8	89.1	89.7	83.3	89.1	89.7	83.3	66.8	89.7	83.3	66.8	89.1	82.2
SKD (Ours)	<u>79.6</u>	93.7	<u>92.7</u>	89.5	93.7	<u>92.9</u>	89.1	81.1	<u>92.6</u>	90.2	81.6	<u>94.2</u>	89.2

the predictions are rather evenly spread among all classes, we adjust the distribution (from y_o to $\tilde{y}_o = \alpha \cdot y_o$) before employing them in the KD-loss (see Fig. 3). In a normal KD setting, the teacher’s winning prediction score usually tends to approach a one-hot vector. The goal is to mimic this distribution while maintaining the relative prediction probabilities. To accomplish that we estimate a factor α so that the mean winning probability equals to τ . We employ a value of $\tau = 0.9$ in our experiments. In the estimation, we equally factor the source and target domain to further maintain the relative prediction confidence between the two domains.

$$\frac{1}{2n_s} \sum_{n_s} \max(\sigma(y_{o,i,s} \cdot \alpha)) + \frac{1}{2n_t} \sum_{n_t} \max(\sigma(y_{o,i,t} \cdot \alpha)) = \tau \quad (2)$$

We then employ the shifted zero-shot predictions for the knowledge distillation loss:

$$L_{KD} = D_{KL}(\tilde{y}_o || y) \quad (3)$$

where D_{KL} is the Kullback-Leibler divergence loss, and y is the output of the classifier of our network.

3.2. Adversarial loss

We employ conditional adversarial domain adaptation loss CDAN:

$$L_{AD} = L_{BCE}(G_d((f_i \otimes p_i), d_i)) \quad (4)$$

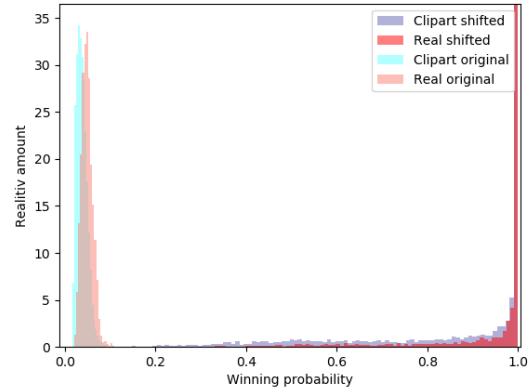


Figure 3. Distribution of winning probabilities of zero-shot predictions y_o and their adjusted distribution \tilde{y}_o for the clipart and real domain of OfficeHome. While the zero-shot predictions have low winning probabilities, the adjusted distribution resembles much more one-hot vectors, while maintaining their relative probabilities, as can be seen from the long tail of low winning probabilities.

where G_d is the domain classification network. f_i are the features of sample i , p_i the class probabilities and d_i the domain label. CDAN employs a gradient reversal layer to inverse the training objective. This means that while the domain classifier is trained to distinguish the domain (source or target) of the respective sample, the objective of the fea-

Table 2. Accuracy results on VisDA dataset. The best results are displayed in bold and the runner-up results are underlined. Methods using a ResNet-101 backbone are on top, and methods using a transformer-based backbone are on the bottom. ZS indicates zero-shot results of CLIP.

Method	plane	bcycl	bus	car	horse	knife	mcycl	person	plant	sktbrd	train	truck	Avg
CDAN [15]	85.2	66.9	83.0	50.8	84.2	74.9	88.1	74.5	83.4	76.0	81.9	38.0	73.9
DWL [31]	90.7	80.2	86.1	67.6	92.4	81.5	86.8	78.1	90.6	57.1	85.6	28.7	77.1
CGDM [3]	93.4	82.7	73.2	68.4	92.9	<u>94.5</u>	88.7	<u>82.1</u>	93.4	82.5	86.8	49.2	82.3
STAR [16]	95.0	84.0	84.6	73.0	91.6	91.8	85.9	78.4	94.4	84.7	87.0	42.2	82.7
CAN [10]	97.0	<u>87.2</u>	82.5	<u>74.3</u>	<u>97.8</u>	96.2	90.8	80.7	96.6	96.3	87.5	59.9	87.2
CoVi [17]	96.8	85.6	88.9	88.6	<u>97.8</u>	93.4	91.9	87.6	<u>96.0</u>	93.8	93.6	48.1	<u>88.5</u>
ZS [22]	98.0	83.3	<u>90.8</u>	65.9	<u>97.8</u>	83.0	<u>93.4</u>	67.7	85.2	90.0	<u>94.9</u>	<u>66.4</u>	84.7
SKD (Ours)	98.8	87.8	92.0	72.0	98.7	93.4	94.8	75.1	92.5	<u>96.0</u>	95.9	72.0	89.1
TVT [34]	82.9	85.6	77.5	60.5	93.6	98.2	89.4	76.4	93.6	92.0	91.7	55.7	83.1
SHOT [14]	99.5	91.8	88.7	65.1	98.6	98.0	96.0	66.1	95.1	<u>98.9</u>	<u>96.8</u>	52.4	87.3
PMTrans [40]	99.4	88.3	88.1	78.9	98.8	<u>98.3</u>	95.8	70.3	94.6	98.3	96.3	48.5	88.0
SSRT [26]	98.9	87.6	89.1	<u>84.8</u>	98.3	98.7	96.3	81.1	94.8	97.9	94.5	43.1	88.8
AdaCon [1]	<u>99.5</u>	<u>94.2</u>	91.2	83.7	98.9	97.7	96.8	71.5	<u>96.0</u>	98.7	97.9	45.0	89.2
DePT-D [6]	99.4	93.8	94.4	87.5	<u>99.4</u>	98.0	<u>96.7</u>	74.3	98.4	98.5	96.6	51.0	<u>90.7</u>
ZS [22]	99.3	91.5	92.9	71.0	<u>99.4</u>	92.7	94.4	75.6	84.7	97.4	95.5	<u>69.0</u>	88.6
SKD (Ours)	99.6	95.2	<u>94.3</u>	74.5	99.6	98.0	95.9	<u>79.8</u>	89.8	99.2	96.6	71.8	91.2

ture extractor is to extract features that are indistinguishable for the domain classifier, thereby generating domain invariant features.

3.3. Gradual source domain expansion

We further employ the gradual source domain expansion strategy [30]. This strategy trains the network iteratively N times, each time resetting the network weights. However, each new run n employs the $\frac{n-1}{N}$ highest scoring target samples with their respective pseudo-labels estimated from the previous run as additional source data. To account for the additional knowledge available from the zero-shot predictions, we slightly modify the algorithm. While the original algorithm only considers the final predictions of the previous run to choose the pseudo-source data, we combine the final predictions with the zero-shot predictions:

$$s(\hat{y}) = p(y_{n-1}) + \frac{1}{2^n} p(\tilde{y}_o) \quad (5)$$

where $s(\hat{y})$ is the scores of the samples for being chosen as pseudo-source samples, and $p(y_{n-1})$ is the final predictions of the previous run. As the performance increases over the runs, we decrease the influence of the zero-shot predictions with every run. We use a value of $N = 5$ in our experiments.

3.4. Batch norm layer adjustment

The ResNet backbone employs batch norm layers. However, the distribution of the pretraining data is vastly dif-

ferent than the data used for the domain adaptation. The running average and mean change abruptly at the beginning of the adaptation process, shifting the data out of the learned distribution and resulting in failure. One solution would be to freeze the batch norm layers, but this can result in exploding feature norms, making the training unstable. In our work, we estimate the average and mean for the source and target data for each batch norm layer and adjust the learnable parameters β and γ so that the running mean and variance equals that of our training data.

$$\tilde{\beta} = \beta - (\mu_p - \mu_c) * \frac{\gamma}{\sqrt{\sigma_p}} \quad (6)$$

$$\tilde{\gamma} = (\gamma * \frac{\sqrt{\sigma_c}}{\sqrt{\sigma_p}}) \quad (7)$$

where μ_p and σ_p represent the running mean and variance of the pre-trained model, and μ_c and σ_c represent the estimated mean and variance of the training data.

4. Experiments

We evaluate our proposed method on three different domain adaptation benchmarks, Office-Home, VisDA, and Domain-Net. We show that we can improve the baselines significantly. In ablation studies, we further investigate the contribution of the different parts of our proposed algorithm.

Table 3. Accuracy results on DomainNet dataset. ZS indicates zero-shot results of CLIP.

MCD [24]	clp	inf	pnt	qdr	rel	skt	Avg	CGDM [3]	clp	inf	pnt	qdr	rel	skt	Avg	MDD [37]	clp	inf	pnt	qdr	rel	skt	Avg
clp	-	15.4	25.5	3.3	44.6	31.2	24.0	clp	-	16.9	35.3	10.8	53.5	36.9	30.7	clp	-	20.5	40.7	6.2	52.5	42.1	32.4
inf	24.1	-	24.0	1.6	35.2	19.7	20.9	inf	27.8	-	28.2	4.4	48.2	22.5	26.2	inf	33.0	-	33.8	2.6	46.2	24.5	28.0
pnt	31.1	14.8	-	1.7	48.1	22.8	23.7	pnt	37.7	14.5	-	4.6	59.4	33.5	30.0	pnt	43.7	20.4	-	2.8	51.2	41.7	32.0
qdr	8.5	2.1	4.6	-	7.9	7.1	6.0	qdr	14.9	1.5	6.2	-	10.9	10.2	8.7	qdr	18.4	3	8.1	-	12.9	11.8	10.8
rel	39.4	17.8	41.2	1.5	-	25.2	25.0	rel	49.4	20.8	47.2	4.8	-	38.2	32.0	rel	52.8	21.6	47.8	4.2	-	41.2	33.5
skt	37.3	12.6	27.2	4.1	34.5	-	23.1	skt	50.1	16.5	43.7	11.1	55.6	-	35.4	skt	54.3	17.5	43.1	5.7	54.2	-	35
Avg	28.1	12.5	24.5	2.4	34.1	21.2	20.5	Avg	36	14	32.1	7.1	45.5	28.3	27.2	Avg	40.4	16.6	34.7	4.3	43.4	32.3	28.6
SCDA [13]	clp	inf	pnt	qdr	rel	skt	Avg	CDTrans [33]	clp	inf	pnt	qdr	rel	skt	Avg	SSRT [26]	clp	inf	pnt	qdr	rel	skt	Avg
clp	-	18.6	39.3	5.1	55	44.1	32.4	clp	-	29.4	57.2	26	72.6	58.1	48.7	clp	-	33.8	60.2	19.4	75.8	59.8	49.8
inf	29.6	-	34	1.4	46.3	25.4	27.3	inf	57	-	54.4	12.8	69.5	48.4	48.4	inf	55.5	-	54	9	68.2	44.7	46.3
pnt	44.1	19	-	2.6	56.2	42	32.8	pnt	62.9	27.4	-	15.8	72.1	53.9	46.4	pnt	61.7	28.5	-	8.4	71.4	55.2	45
qdr	30.0	4.9	15	-	25.4	19.8	19	qdr	44.6	8.9	29	-	42.6	28.5	30.7	qdr	42.5	8.8	24.2	-	37.6	33.6	29.3
rel	54	22.5	51.9	2.3	-	42.5	34.6	rel	66.2	31	61.5	16.2	-	52.9	45.6	rel	69.9	37.1	66	10.1	-	58.9	48.4
skt	55.6	18.5	44.7	6.4	53.2	-	35.7	skt	69	29.6	59	27.2	72.5	-	51.5	skt	70.6	32.8	62.2	21.7	73.2	-	52.1
Avg	42.6	16.7	37	3.6	47.2	34.8	30.3	Avg	59.9	25.3	52.2	19.6	65.9	48.4	45.2	Avg	60	28.2	53.3	13.7	65.3	50.4	45.2
PMTrans [40]	clp	inf	pnt	qdr	rel	skt	Avg	ZS [22]	clp	inf	pnt	qdr	rel	skt	Avg	SKD (Ours)	clp	inf	pnt	qdr	rel	skt	Avg
clp	-	34.2	62.7	32.5	79.3	63.7	54.5	clp	-	48.3	68.5	14.0	84.6	65.8	56.3	clp	-	52.7	72.0	36.3	85.1	71.5	63.5
inf	67.4	-	61.1	22.2	78	57.6	57.3	inf	73.1	-	68.5	14.0	84.6	65.8	61.2	inf	78.5	-	72.2	30.4	85.0	69.5	67.1
pnt	69.7	33.5	-	23.9	79.8	61.2	53.6	pnt	73.1	48.3	-	14.0	84.6	65.8	57.2	pnt	78.7	49.8	-	29.6	84.5	69.7	62.4
qdr	54.6	17.4	38.9	-	49.5	41	40.3	qdr	73.1	48.3	68.5	-	84.6	65.8	68.1	qdr	70.7	22.9	50.9	-	82.4	62.3	57.8
rel	74.1	35.3	70	25.4	-	61.1	53.2	rel	73.1	48.3	68.5	14.0	-	65.8	54.0	rel	80.3	53.5	74.2	30.2	-	71.1	61.9
skt	73.8	33.0	62.6	30.9	77.5	-	55.6	skt	73.1	48.3	68.5	14.0	84.6	-	57.7	skt	81.0	52.0	73.0	36.6	84.6	-	65.4
Avg	67.9	30.7	59.1	27	72.8	56.9	52.4	Avg	73.1	48.3	68.5	14.0	84.6	65.8	59.1	Avg	77.9	46.2	68.5	32.6	84.3	68.8	63.0

4.1. Setup

Office-Home [28] contains 15,500 images of 65 categories. The domains are Art (A), Clipart (C), Product (P), and Real-World (R). We evaluate all twelve possible adaptation tasks.

VisDA [18] is a challenging dataset for synthetic-to-real domain adaptation. The synthetic source domain consists of 152397 images and the real-world target domain consists of 55388 images over 12 different classes.

DomainNet [19] is a large-scale dataset with about 600,000 images from 6 different domains and 345 different classes. We evaluate all 30 possible adaptation tasks.

Implementation details: We built up our implementation on the CDAN implementation of [15]. We do all experiments with the CLIP-trained versions of the ResNet backbone and transformer backbone. For the ResNet backbone, we follow most other publications and employ ResNet-50 for OfficeHome and ResNet-101 for VisDA. For the transformer backbone, we employ ViT-B/16. We employ the seven ImageNet templates subset published on the CLIP Git Hub for the language encoder to estimate the zero-shot predictions. For OfficeHome we train each run for 100 episodes, for VisDA and DomainNet we train for 50 episodes. For OfficeHome and DomainNet, we employ AdamW optimizer with a learning rate of $5e^{-6}$ for the backbone and $5e^{-5}$ for the newly initialized layers. For VisDA we employ a lower learning rate of $1e^{-6}$, and $1e^{-5}$ respectively. We employ the GSDE strategy for a total of $N = 5$ runs. Each experiment is run for three different seeds, except for the DomainNet which we only train for one seed.

4.2. Results

Results for Office-Home: The results for the Office-Home dataset are shown in Tab. 1. The zero-shot predictions al-

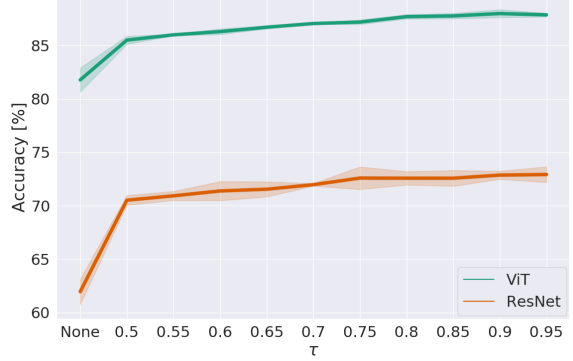


Figure 4. Accuracy for adaptation of OfficeHome C→A for different values for τ . None represents directly using the zero-shot predictions without any distribution shift. It can be seen that adjusting the probability distribution is fundamental for the knowledge distillation to work properly.

ready outperform some of the earlier works but are considerably below current state-of-the-art algorithms. Using our method, we improve the average accuracy by 7.3pp for the ResNet-50 backbone and 7.0pp for the ViT backbone. An improvement can be seen for all 12 adaptation tasks. For the ResNet backbone, we improve the state-of-the-art by around 4.3pp.

Results for VisDA-2017: The results for the VisDA-2017 dataset are shown in Tab. 2. Again, the zero-shot predictions already outperform some of the earlier works but are considerably below current state-of-the-art algorithms. Using our method, we improve the average accuracy by 4.4pp for the ResNet-101 backbone and 2.6pp for the ViT backbone, letting us outperform current state-of-the-art methods.

Table 4. Contributions of different parts of our algorithm. Aug means using strongly augmented images alongside the weakly augmented ones, while GSDE uses only the prediction scores of the previous run, GSDE+ adds zero-shot prediction scores according to eq. 5.

L_{AD}	L_{KD}	Aug	GSDE	GSDE+	ResNet		ViT	
					VisDA	OH	VisDA	OH
✓					72.73	65.99	74.25	81.74
	✓				87.65	69.06	90.28	83.27
✓	✓				88.21	73.43	90.44	87.66
✓	✓	✓			88.62	75.48	90.37	87.97
✓	✓	✓	✓		88.90	78.72	91.22	89.08
✓	✓	✓		✓	89.09	78.78	91.20	89.24

Table 5. Generalization to unseen data.

	train	test	comb
ZS	59.05	59.11	59.07
Ours	63.32	62.38	63.04

Results for DomainNet: The results for the DomainNet dataset are shown in Tab. 3. The zero-shot predictions already outperform current state-of-the-art methods considerably. By using our method we further increase the average accuracy by 3.9pp. We achieve the biggest increase of performance over the zero-shot predictions for the target set of quickdraw, increasing the accuracy by 18.6pp. However, when using the quickdraw domain as source data, the accuracy decreases considerably by around 10.3pp compared to the zero-shot predictions. The quickdraw domain has a large domain gap to the other domains. This large gap introduces a negative transfer resulting in a drop in accuracy.

5. Ablation studies

Parameter for adjusting zero-shot distribution τ : In this part, we evaluate the effect of the parameter τ . Figure 4 shows the accuracy for different values of τ . None means that no distribution shift was applied to the zero-shot predictions. It can be seen that applying the distribution shift is essential for the method. Employing a shift of $\tau = 0.9$ increases the accuracy by 10.9pp for ResNet and 6.2pp for ViT backbone. For the ViT backbone, the accuracy increases constantly until a value of 0.9, for which the accuracy peaks. For the ResNet backbone, it seems that even higher values of τ yield better results. In all our experiments, we employ a value for τ of 0.9.

Contribution of losses: In this part, we evaluate the contribution of the different losses to our method. The combination of L_{AD} and L_{KD} improves the accuracy in all of the four settings. Especially for the OfficeHome dataset, where adversarial domain adaptation and knowledge distillation achieve similar results, the boost is the largest. Data

augmentation further slightly increases the accuracy. And we achieve another boost by introducing GSDE. Introducing the zero-shot predictions into the GSDE algorithm increases the accuracy further a slight bit.

Generalization to unseen data: Since we only used the training sets for the adaptation task in the DomainNet dataset, it allows us to evaluate the generalization ability to unseen data. The results are shown in Tab. 5. As expected the zero-shot accuracy is similar between the train and test set. Our method has a slight drop of around 1pp for the test set, meaning that there is a slight overfitting to the seen data. However it still significantly outperforms the zero-shot prediction accuracy. Since the train dataset is much larger than the test dataset, the combined results are closer to the train dataset.

T-SNE visualization: We visualize the feature embedding using T-SNE for the addition of the different losses as well as for the CLIP pre-trained model in 5. Since the CLIP model is not trained classification but aligning visual and language features, the distribution is very spread out (see Fig. 5a). Interestingly the source and target domain are quite separated. Using the KD loss (and classification loss) aligns the different classes into clusters, but does not do a good job of aligning the features (see Fig. 5c). The CDAN loss aligns both domains well but suffers from misalignment between different classes (see Fig. 5e). By combining the two methods, we get well-aligned domains with fewer misalignments (see Fig. 5g).

6. Discussion

In this work, we presented a novel way to combine the knowledge of vision-language models with knowledge gained from a source dataset through unsupervised domain adaptation. We maintain the inherent knowledge of the vision-language model via a knowledge distillation loss. To effectively distill the knowledge we introduced a distribution adjustment for the prediction probabilities. For the domain adaptation loss, we employed CDAN as it is effective for both CNN and transformer-based backbones. We showed the effectiveness of our method for both backbones

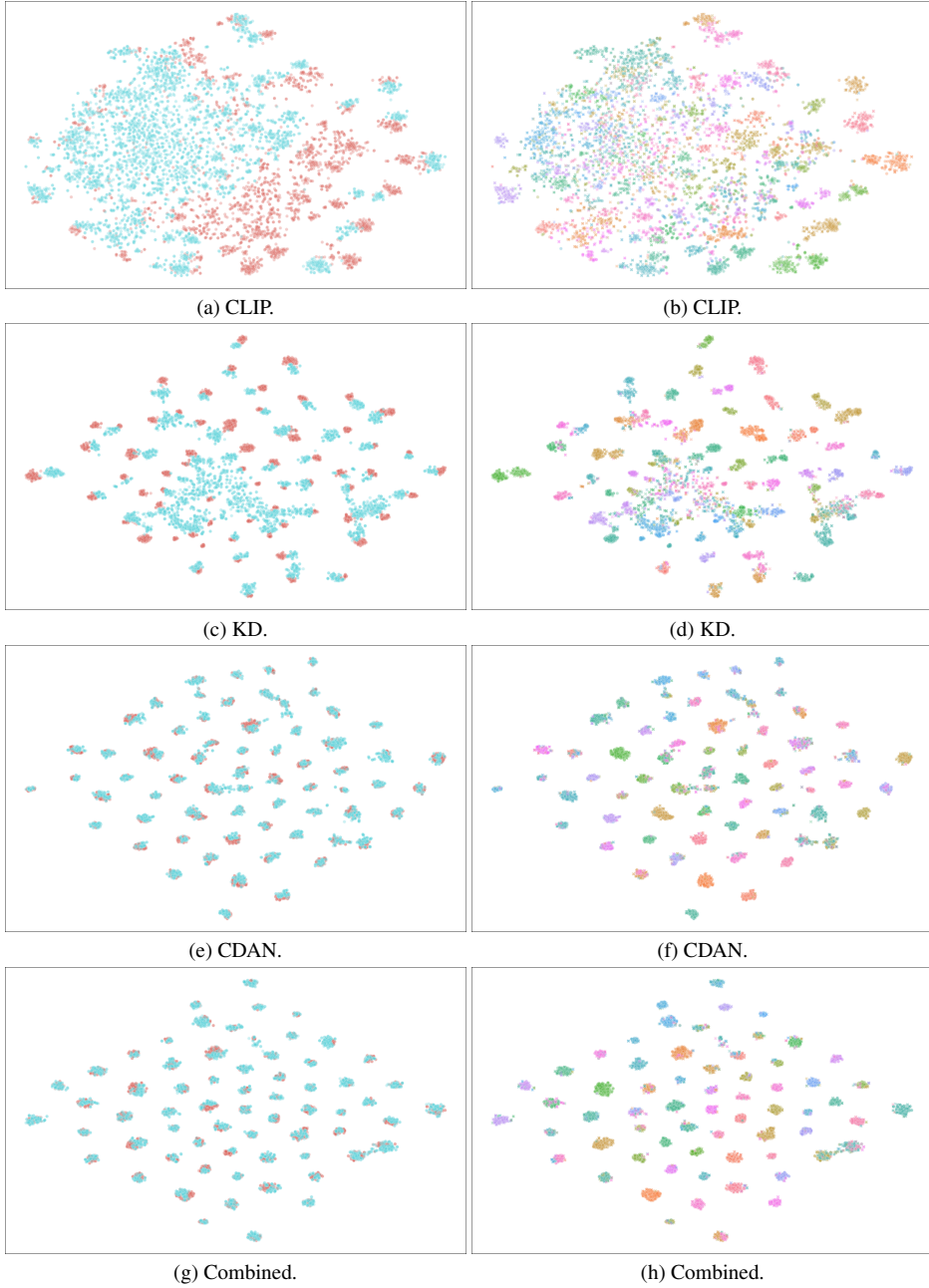


Figure 5. TSNE visualization of the A→C adaptation task. On the left side source samples are in red, and target ones are in blue. On the right side source samples are marked by circles and target ones by crosses.

on three different datasets, outperforming current state-of-the-art methods. We showed that combining unsupervised domain adaptation with the inherent knowledge of vision-language models improves the performance significantly over using only one of the knowledge sources. It should be stated, that it can be expected to further increase the performance by choosing a stronger method for the domain adaptation task.

Acknowledgment

This work was partially supported by JST Moonshot R&D Grant Number JPMJPS2011, CREST Grant Number JP-MJCR2015, JSPS KAKENHI Grant Number JP21K17799, and Basic Research Grant (Super AI) of Institute for AI and Beyond of the University of Tokyo.

References

[1] Dian Chen, Dequan Wang, Trevor Darrell, and Sayna Ebrahimi. Contrastive test-time adaptation. In *Proceedings of the IEEE/CVF Conference on Computer Vision and Pattern Recognition*, pages 295–305, 2022. 5

[2] Haoran Chen, Zuxuan Wu, Xintong Han, and Yu-Gang Jiang. Multi-prompt alignment for multi-source unsupervised domain adaptation. *arXiv preprint arXiv:2209.15210*, 2022. 3

[3] Zhekai Du, Jingjing Li, Hongzu Su, Lei Zhu, and Ke Lu. Cross-domain gradient discrepancy minimization for unsupervised domain adaptation. In *Proceedings of the IEEE/CVF conference on computer vision and pattern recognition*, pages 3937–3946, 2021. 5, 6

[4] Alex Fang, Albin Madappally Jose, Amit Jain, Ludwig Schmidt, Alexander Toshev, and Vaishaal Shankar. Data filtering networks. *arXiv preprint arXiv:2309.17425*, 2023. 2

[5] Yaroslav Ganin, Evgeniya Ustinova, Hana Ajakan, Pascal Germain, Hugo Larochelle, François Laviolette, Mario Marchand, and Victor Lempitsky. Domain-adversarial training of neural networks. *The journal of machine learning research*, 17(1):2096–2030, 2016. 2

[6] Yunhe Gao, Xingjian Shi, Yi Zhu, Hao Wang, Zhiqiang Tang, Xiong Zhou, Mu Li, and Dimitris N Metaxas. Visual prompt tuning for test-time domain adaptation. *arXiv preprint arXiv:2210.04831*, 2022. 5

[7] Chunjiang Ge, Rui Huang, Mixue Xie, Zihang Lai, Shiji Song, Shuang Li, and Gao Huang. Domain adaptation via prompt learning. *arXiv preprint arXiv:2202.06687*, 2022. 3

[8] Geoffrey Hinton, Oriol Vinyals, and Jeff Dean. Distilling the knowledge in a neural network. *arXiv preprint arXiv:1503.02531*, 2015. 3

[9] Chao Jia, Yinfei Yang, Ye Xia, Yi-Ting Chen, Zarana Parekh, Hieu Pham, Quoc Le, Yun-Hsuan Sung, Zhen Li, and Tom Duerig. Scaling up visual and vision-language representation learning with noisy text supervision. In *International conference on machine learning*, pages 4904–4916. PMLR, 2021. 2

[10] Guoliang Kang, Lu Jiang, Yi Yang, and Alexander G Hauptmann. Contrastive adaptation network for unsupervised domain adaptation. In *Proceedings of the IEEE/CVF conference on computer vision and pattern recognition*, pages 4893–4902, 2019. 5

[11] Donghyun Kim, Kaihong Wang, Stan Sclaroff, and Kate Saenko. A broad study of pre-training for domain generalization and adaptation. In *ECCV*, pages 621–638. Springer, 2022. 2, 3

[12] Junjie Li, Yixin Zhang, Zilei Wang, and Keyu Tu. Probabilistic contrastive learning for domain adaptation. *arXiv preprint arXiv:2111.06021*, 2021. 4

[13] Shuang Li, Mixue Xie, Fangrui Lv, Chi Harold Liu, Jian Liang, Chen Qin, and Wei Li. Semantic concentration for domain adaptation. In *Proceedings of the IEEE/CVF international conference on computer vision*, pages 9102–9111, 2021. 6

[14] Jian Liang, Dapeng Hu, and Jiashi Feng. Do we really need to access the source data? source hypothesis transfer for unsupervised domain adaptation. In *International Conference on Machine Learning*, pages 6028–6039. PMLR, 2020. 2, 5

[15] Mingsheng Long, Zhangjie Cao, Jianmin Wang, and Michael I. Jordan. Conditional adversarial domain adaptation. In *NeurIPS*, pages 1647–1657, 2018. 2, 4, 5, 6

[16] Zhihe Lu, Yongxin Yang, Xiatian Zhu, Cong Liu, Yi-Zhe Song, and Tao Xiang. Stochastic classifiers for unsupervised domain adaptation. In *Proceedings of the IEEE/CVF Conference on Computer Vision and Pattern Recognition*, pages 9111–9120, 2020. 5

[17] Jaemin Na, Dongyoon Han, Hyung Jin Chang, and Wonjun Hwang. Contrastive vicinal space for unsupervised domain adaptation. In *European Conference on Computer Vision*, pages 92–110. Springer, 2022. 5

[18] Xingchao Peng, Ben Usman, Neela Kaushik, Judy Hoffman, Dequan Wang, and Kate Saenko. Visda: The visual domain adaptation challenge. *arXiv preprint arXiv:1710.06924*, 2017. 6

[19] Xingchao Peng, Qinxun Bai, Xide Xia, Zijun Huang, Kate Saenko, and Bo Wang. Moment matching for multi-source domain adaptation. In *ICCV*, pages 1406–1415, 2019. 6

[20] Hieu Pham, Zihang Dai, Golnaz Ghiasi, Kenji Kawaguchi, Hanxiao Liu, Adams Wei Yu, Jiahui Yu, Yi-Ting Chen, Minh-Thang Luong, Yonghui Wu, et al. Combined scaling for zero-shot transfer learning. *Neurocomputing*, 555:126658, 2023. 2

[21] Viraj Prabhu, Shivam Khare, Deeksha Kartik, and Judy Hoffman. Sentry: Selective entropy optimization via committee consistency for unsupervised domain adaptation. In *Proceedings of the IEEE/CVF International Conference on Computer Vision*, pages 8558–8567, 2021. 2, 4

[22] Alec Radford, Jong Wook Kim, Chris Hallacy, Aditya Ramesh, Gabriel Goh, Sandhini Agarwal, Girish Sastry, Amanda Askell, Pamela Mishkin, Jack Clark, et al. Learning transferable visual models from natural language supervision. In *International conference on machine learning*, pages 8748–8763. PMLR, 2021. 2, 4, 5, 6

[23] Harsh Rangwani, Sumukh K Aithal, Mayank Mishra, Arishant Jain, and Venkatesh Babu Radhakrishnan. A closer look at smoothness in domain adversarial training. In *International Conference on Machine Learning*, pages 18378–18399. PMLR, 2022. 4

[24] Kuniaki Saito, Kohei Watanabe, Yoshitaka Ushiku, and Tatsuya Harada. Maximum classifier discrepancy for unsupervised domain adaptation. In *Proceedings of the IEEE conference on computer vision and pattern recognition*, pages 3723–3732, 2018. 6

[25] Mainak Singha, Harsh Pal, Ankit Jha, and Biplab Banerjee. Ad-clip: Adapting domains in prompt space using clip. In *Proceedings of the IEEE/CVF International Conference on Computer Vision*, pages 4355–4364, 2023. 3

[26] Tao Sun, Cheng Lu, Tianshuo Zhang, and Haibin Ling. Safe self-refinement for transformer-based domain adaptation. In *Proceedings of the IEEE/CVF conference on computer vision and pattern recognition*, pages 7191–7200, 2022. 4, 5, 6

[27] Hui Tang, Ke Chen, and Kui Jia. Unsupervised domain adaptation via structurally regularized deep clustering. In *Proceedings of the IEEE/CVF conference on computer vision and pattern recognition*, pages 8725–8735, 2020. 4

[28] Hemanth Venkateswara, Jose Eusebio, Shayok Chakraborty, and Sethuraman Panchanathan. Deep hashing network for unsupervised domain adaptation. In *CVPR*, pages 5018–5027, 2017. 6

[29] Thomas Westfertel, Hao-Wei Yeh, Qier Meng, Yusuke Mukuta, and Tatsuya Harada. Backprop induced feature weighting for adversarial domain adaptation with iterative label distribution alignment. In *Proceedings of the IEEE/CVF Winter Conference on Applications of Computer Vision*, pages 392–401, 2023. 4

[30] Thomas Westfertel, Hao-Wei Yeh, Dexuan Zhang, and Tatsuya Harada. Gradual source domain expansion for unsupervised domain adaptation. *arXiv preprint arXiv:2311.09599*, 2023. 2, 4, 5

[31] Ni Xiao and Lei Zhang. Dynamic weighted learning for unsupervised domain adaptation. In *Proceedings of the IEEE/CVF conference on computer vision and pattern recognition*, pages 15242–15251, 2021. 5

[32] Shaoan Xie, Zibin Zheng, Liang Chen, and Chuan Chen. Learning semantic representations for unsupervised domain adaptation. In *International conference on machine learning*, pages 5423–5432. PMLR, 2018. 2

[33] Tongkun Xu, Weihua Chen, Pichao Wang, Fan Wang, Hao Li, and Rong Jin. Cdtrans: Cross-domain transformer for unsupervised domain adaptation. *arXiv preprint arXiv:2109.06165*, 2021. 2, 4, 6

[34] Jinyu Yang, Jingjing Liu, Ning Xu, and Junzhou Huang. Tvt: Transferable vision transformer for unsupervised domain adaptation. In *Proceedings of the IEEE/CVF Winter Conference on Applications of Computer Vision*, pages 520–530, 2023. 2, 4, 5

[35] Giacomo Zara, Alessandro Conti, Subhankar Roy, Stéphane Lathuilière, Paolo Rota, and Elisa Ricci. The unreasonable effectiveness of large language-vision models for source-free video domain adaptation. In *Proceedings of the IEEE/CVF International Conference on Computer Vision*, pages 10307–10317, 2023. 3

[36] Xiaohua Zhai, Xiao Wang, Basil Mustafa, Andreas Steiner, Daniel Keysers, Alexander Kolesnikov, and Lucas Beyer. Lit: Zero-shot transfer with locked-image text tuning. In *Proceedings of the IEEE/CVF Conference on Computer Vision and Pattern Recognition*, pages 18123–18133, 2022. 2

[37] Yuchen Zhang, Tianle Liu, Mingsheng Long, and Michael Jordan. Bridging theory and algorithm for domain adaptation. In *International Conference on Machine Learning*, pages 7404–7413. PMLR, 2019. 6

[38] Sicheng Zhao, Xiangyu Yue, Shanghang Zhang, Bo Li, Han Zhao, Bichen Wu, Ravi Krishna, Joseph E Gonzalez, Alberto L Sangiovanni-Vincentelli, Sanjit A Seshia, et al. A review of single-source deep unsupervised visual domain adaptation. *IEEE Transactions on Neural Networks and Learning Systems*, 33(2):473–493, 2020. 2

[39] Kaiyang Zhou, Jingkang Yang, Chen Change Loy, and Ziwei Liu. Learning to prompt for vision-language models. In *International Journal of Computer Vision*, 130(9):2337–2348, 2022. 3

[40] Jinjing Zhu, Haotian Bai, and Lin Wang. Patch-mix transformer for unsupervised domain adaptation: A game perspective. In *Proceedings of the IEEE/CVF Conference on Computer Vision and Pattern Recognition*, pages 3561–3571, 2023. 2, 4, 5, 6

[41] Fuzhen Zhuang, Zhiyuan Qi, Keyu Duan, Dongbo Xi, Yongchun Zhu, Hengshu Zhu, Hui Xiong, and Qing He. A comprehensive survey on transfer learning. *Proceedings of the IEEE*, 109(1):43–76, 2020. 2